

Prediction of Blast Loads on a Deformable Steel Plate Using Euler Equations

Emre Alpman*

Marmara University, Istanbul, Turkey, 34722

Lyle N. Long[†], Chien-Chung Chen[‡], and Daniel G. Linzell[§]
The Pennsylvania State University, University Park, PA, 16802.

The in-house computational fluid dynamics code PUMA2 was used to predict blast loads on a steel plate. In this study PUMA2 has been modified to include high temperature effects for air at equilibrium conditions in addition to the calorically perfect gas assumption. Preliminary tests performed for a planar shock wave and square cavity interaction agreed well with the experimental results. A blast simulation performed with the calorically perfect gas assumption in free air successfully predicted peak pressures with reasonable accuracy at various distances and qualitatively yielded the typical behavior of spherical blast waves. Finally blast loadings on a steel plate were predicted using calorically perfect gas and equilibrium air assumptions. Peak pressures yielded by these two solutions were similar and agreed well with predictions from the A.T.-Blast program, while the peak temperature predictions were quite different. Blast loads were used as input loads for the LS-DYNA finite element analysis code to investigate the effects of coating a steel plate using polyurea. Simulations performed for a steel plate with and without polyurea coating appear to demonstrate its effectiveness against fragmentation and failure due to air blast effects.

Nomenclature

c	=	local speed of sound
E	=	total energy per unit mass
H	=	total enthalpy per unit mass
p	=	static pressure
P_s	=	over-pressure
t	=	time
T	=	temperature
u_i	=	flow velocity vector
V_r	=	radial flow velocity
x_i	=	Cartesian coordinates
γ	=	ratio of specific heats
ρ	=	air density

I. Background

Predicting the effects of blast waves on solid structures is a very important step in designing safe structures and vehicles for civilians and military personnel to protect them from any explosions that might occur. Research in this area has mainly focused on experimental studies which involve the detonation of real explosives and investigating the effects of the blast impact on structures which are built for these experiments. Such experiments are not only very dangerous but also are very expensive to perform. Moreover, if there is substantial amount of explosive involved then federal regulations allow only the military to perform such experiments. An alternative to

*Assistant Professor, Mechanical Engineering Department, Goztepe Campus, Kadikoy, Istanbul, Turkey, 34722

[†]Distinguished Professor, Aerospace Engineering Department, University Park, PA, 16802, AIAA Fellow.

[‡]Graduate Research Assistant, Civil and Environmental Engineering Department, University Park, PA, 16802.

[§]Associate Professor, Civil and Environmental Engineering Department, University Park, PA, 16802.

the experimental techniques is a computational approach, where blast impact simulations are performed using computers. This approach is much more feasible and one can also avoid the dangers associated with handling explosives.

Physically a detonation can be defined as a shock wave generated due to the energy release of an exothermic reaction¹. When a uniform detonation occurs, the resulting high pressure and high temperature gases expand into the ambient air and produce a spherical shock wave². Therefore, a numerical method that is to be used for blast wave simulations must involve sufficient physics to handle moving spherical shock waves and their reflections from any solid surface. In addition to this, a numerical solver for this problem must also be fast enough to produce results quickly. Sharma and Long used the Direct Simulation Monte Carlo (DSMC) method to simulate the blast impact problem³. DSMC is a particle simulation method based on kinetic theory of gases. It is originally designed for rarefied gas dynamics problems and is a very powerful tool to model detonations and flows with chemical reactions⁴⁻⁷. But being designed for rarefied gas dynamics, DSMC can be very expensive for flow simulations over large distances in continuum atmospheres. Assuming local thermodynamic equilibrium could make DSMC much more economical for continuum flows⁸. But this assumption makes the method equivalent to solving Euler equations². Therefore, in this study Euler equations were used to define the flowfield. An Euler/Navier-Stokes solver PUMA2 is employed to simulate the evolution blast waves and interactions with a square plate. The code predicts the resultant pressure loadings on the plate which can be used as an input to the structural dynamics codes such as LS-DYNA⁹ to determine the stress and displacements. In this manner the computational fluid dynamics (CFD) code and the structural dynamics code are loosely coupled. In reality, the deformations on the plate may affect the shock structure and change the pressure loading, but we believe that the loosely coupled solutions are sufficient for the initial design purposes.

II. Objective

This paper presents simulations of blast waves generated due to explosions in free air and in the vicinity of a square uncoated or coated (with polyurea) steel plate. The pressure loadings obtained by the CFD code were used as input for the explicit finite element analysis code LS-DYNA⁹, which computed resulting stresses and strains and modes of failure of the plate. Results are intended to be used to investigate the effectiveness of polyurea for mitigating blast effects on steel components.

III. Computer Code PUMA2

Numerical solutions were obtained using the computer code PUMA2 (Parallel Unstructured Maritime Aerodynamics-2), which is an in-house computational fluid dynamics code written in ANSI C++. It was designed for the analysis of external, non-reacting compressible flow over three-dimensional geometries. The original version of the code (PUMA) was developed by Bruner¹⁰. PUMA2 solves the full Navier-Stokes equations using a finite volume technique and supports several unstructured grid topologies. Numerous improvements have been made to PUMA2 by Long et. al¹¹⁻²⁶.

For the blast simulations, the viscous effects of the flow are neglected and numerical predictions are obtained by solving the Euler equations. The Euler equations, which are the mass, momentum and energy conservation equations, can be written as follows:

$$\frac{\partial \rho}{\partial t} + \frac{\partial \rho u_i}{\partial x_i} = 0 \quad (1)$$

$$\frac{\partial \rho u_i}{\partial t} + \frac{\partial \rho u_i u_j}{\partial x_j} + \frac{\partial p}{\partial x_i} = 0 \quad (2)$$

$$\frac{\partial \rho E}{\partial t} + \frac{\partial \rho u_i H}{\partial x_i} = 0 \quad (3)$$

Where ρ is the fluid density, u_i is the velocity vector, p is the static pressure, E and H are total energy and total enthalpy per unit mass.

$$E = \frac{p}{\rho(\gamma - 1)} + \frac{u_i u_i}{2} \quad (4)$$

$$H = E + \frac{p}{\rho} \quad (5)$$

For a calorically perfect gas, γ , the ratio of specific heats is constant at a value of 1.4. But in blast simulation problems, a detonation may lead to very high temperatures which may cause gas dissociation and invalidates the calorically perfect gas assumption. Then, the well known relations for temperature and local speed of sound given in equations (6) and (7) also cease to be valid.

$$p = \rho R T \quad (6)$$

$$c = \sqrt{\frac{\gamma p}{\rho}} \quad (7)$$

Since the calorically perfect gas assumption does not take in to account chemical reactions, it can yield unrealistically high temperatures²⁷. Therefore, gas dissociation effects must sometimes be included to the equations for correct predictions. In this study local chemical equilibrium was assumed stating that the chemical reactions occur so fast that local equilibrium is reached instantaneously²⁷. This assumption yields good results unless the air density is very low²⁸. For equilibrium air properties the relations given in Ref. 29 were used to compute γ , temperature and local speed of sound in terms of pressure and density.

In PUMA2 the equations (1), (2), and (3) are numerically solved using a finite volume technique which breaks up the computational domain into control volumes. The fluxes at the cell faces are computed using Roe's flux difference splitting scheme³⁰. Since Roe's scheme was originally designed using the calorically perfect gas assumption, the AUSM⁺ method³¹, which is suitable for Euler Equations with variable γ , was used for flow solutions with high temperature effects.

IV. Results

A. Interaction of a Planar Shock with a Square Cavity

Since the blast impact problem is a simply a shock wave/solid surface interaction problem, the code was first tested for interaction of a planar shock wave with a square cavity. This problem was first investigated experimentally and numerically by Igra et. al³². Figure 1 shows the sectional view of the computational mesh generated for the numerical solutions. The mesh is composed of 1.4 million tetrahedral cells. Here the planar shock moves from left to right with a Mach number of 1.3.

Figures 2, 3, and 4 show density contours obtained at different times with Roe's scheme and AUSM⁺. These predictions are in good agreement with the shadowgraphs from Ref. 32. AUSM⁺ provided sharper shocks and better predictions especially where the shock strength is low.

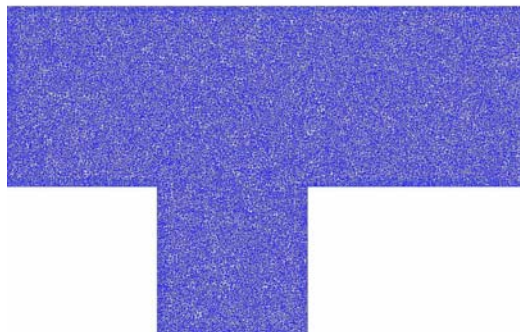


Figure 1. Sectional view of the computational mesh.

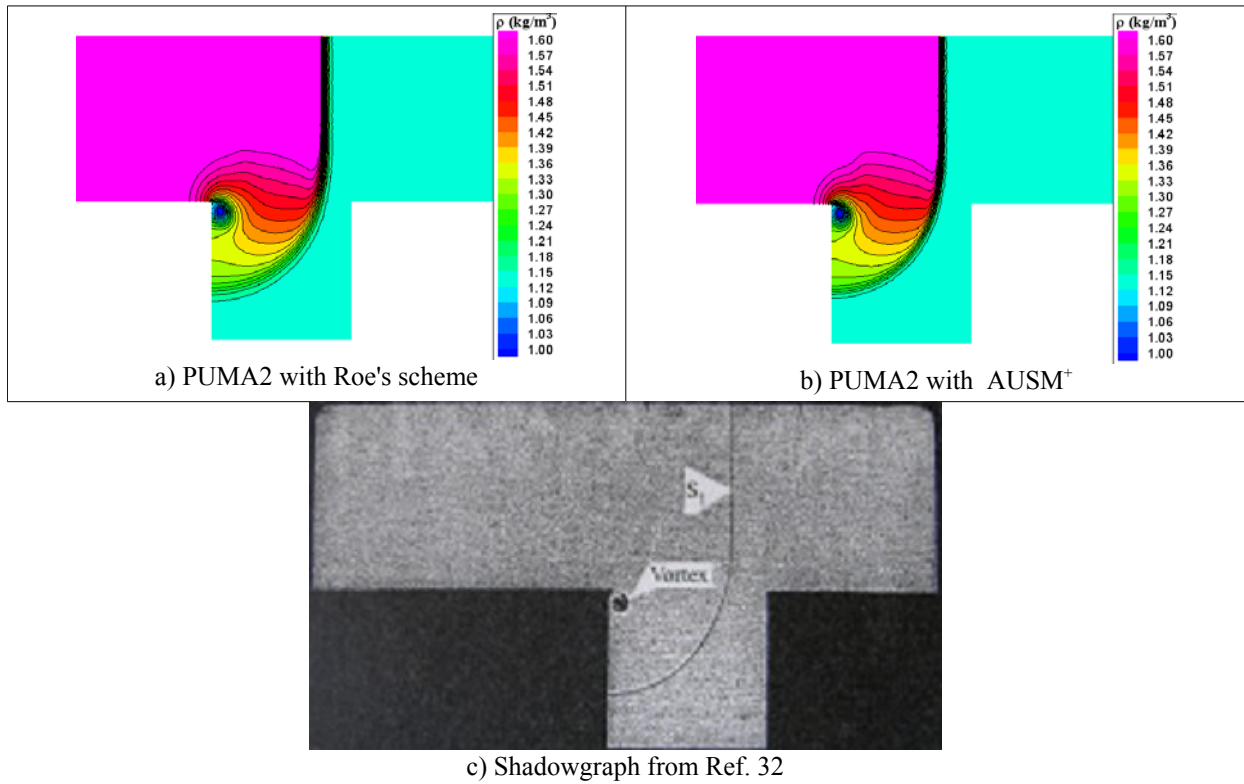


Figure 2. Interaction of a planar shock with a square cavity (density contours, $M_s = 1.3$), $t = 100 \mu s$

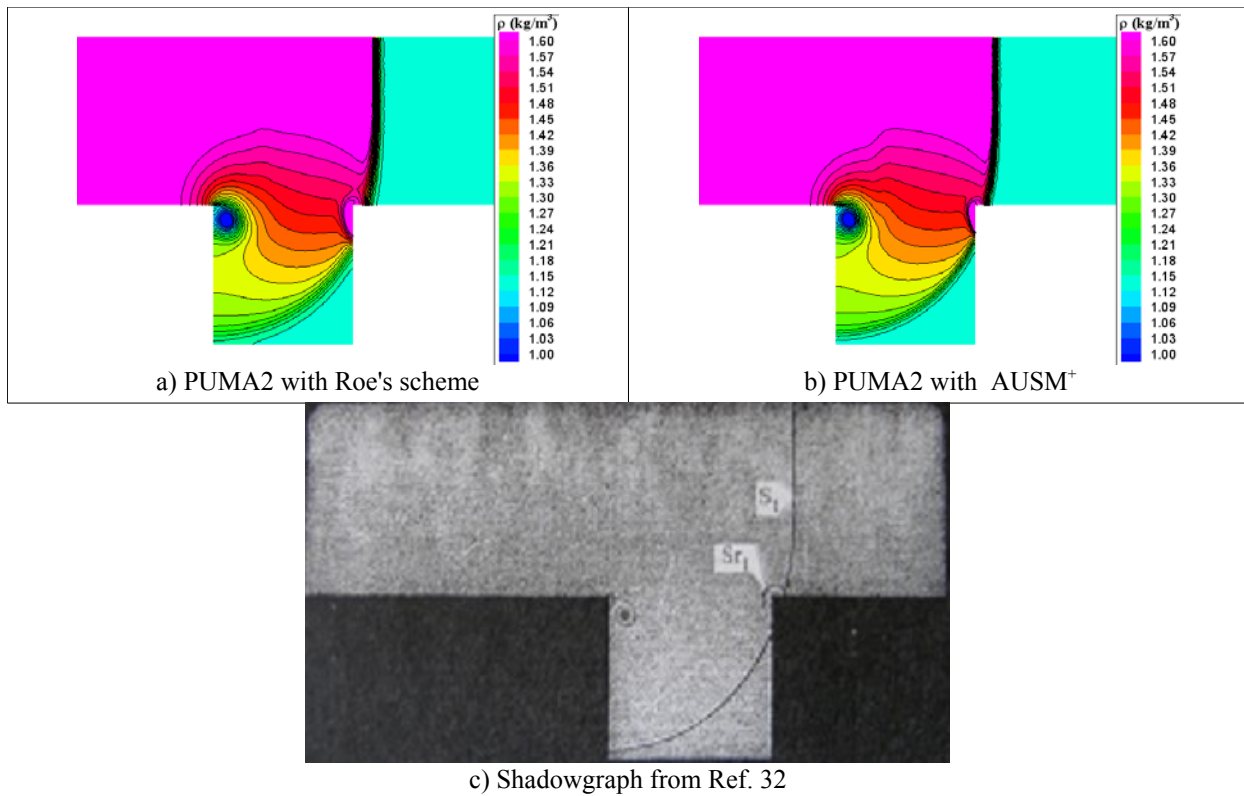


Figure 3. Interaction of a planar shock with a square cavity (density contours, $M_s = 1.3$), $t = 140 \mu s$

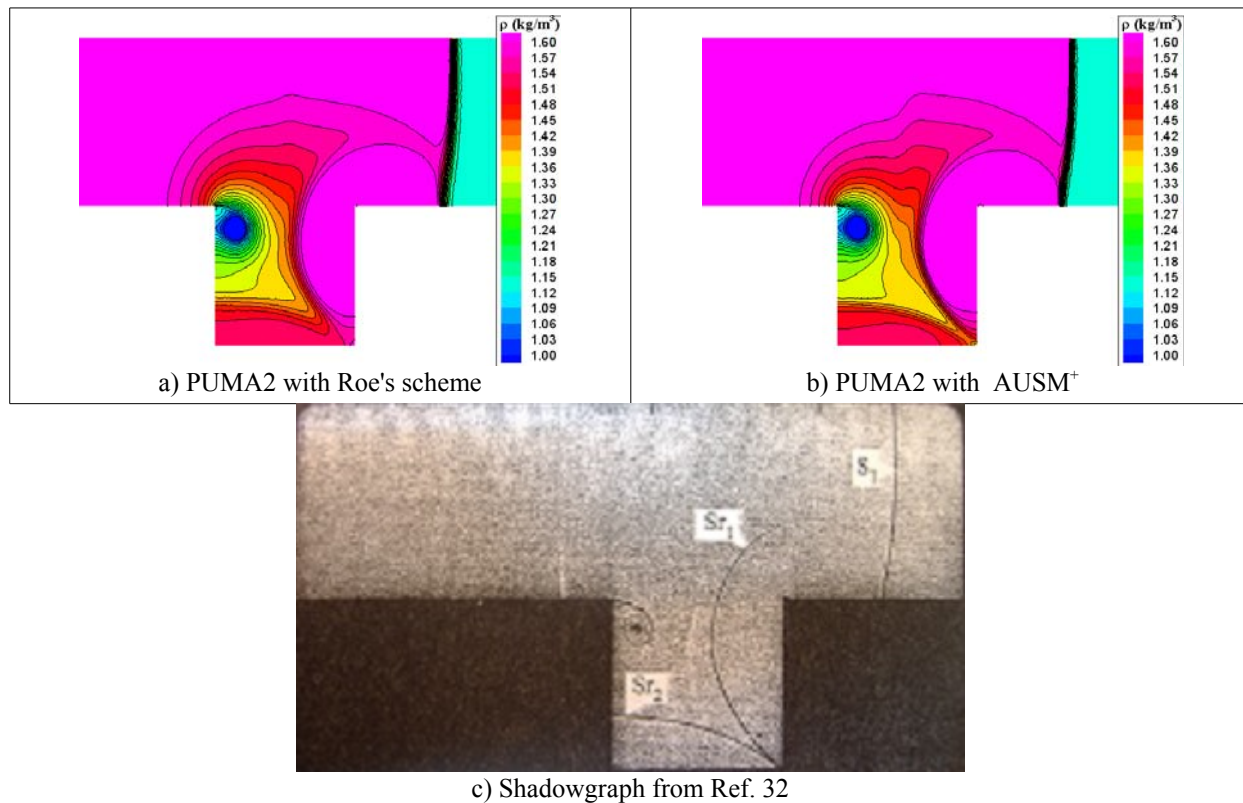


Figure 4. Interaction of a planar shock with a square cavity (density contours, $M_s = 1.3$), $t = 200 \mu s$

B. Simulation of a Blast Wave in Free Air

In this section the evolution of a blast wave generated by the explosion of 75 lbs of TNT was simulated. In the solution, the explosive was assumed to be spherical in shape, and the density of TNT is taken as 1500 kg/m^3 . The simulations start after the detonation wave reaches the surface of the explosive, therefore the blast effects were introduced into the code as initial conditions for pressure, density and radial velocity. This means that the initial conditions for PUMA2 are for a spherical blast wave that has already traveled a short distance from detonation center. These initial conditions were taken from Ref. 33. During the solutions high temperature effects were neglected and air is treated as a calorically perfect gas. Moreover, the presence of TNT products was also omitted for simplicity. Figure 5 shows the variation of over-pressure with scaled distance, Z . Here the scaled distance was computed as the distance from the center of the explosive divided by the cubic root of its weight. The predictions were also compared with the results presented in Ref. 34. Ref. 34 adapted these data from number references including the US Army design code TM5-1300. Despite the calorically perfect gas assumption, PUMA2 was able to predict the over-pressure distribution in a good agreement with the distribution given in Ref. 34. This is a very encouraging result to show the effectiveness of the code to predict blast loadings.

A blast wave from a spherical charge problem was investigated by Brode³⁵. His computations showed that after the main shock wave a secondary shock occurs which moves outward for a time and then implodes on the origin and then reflected outwards. Such a behavior can be observed in Figure 6 where variation of radial velocity, predicted by PUMA2, with distance from the explosive center is displayed at different times. This figure clearly shows a secondary shock wave develops after the primary one. It moves forward for a while and then implodes and is reflected from the origin.

Figure 7 shows the pressure profile at the scaled distance $Z = 1$ ($\sim 3.24 \text{ m}$). Typically, for a blast wave in free air, the positive pressure phase is followed by a negative pressure phase where the static pressure drops below the ambient pressure. Such a behavior is clearly visible in this figure.

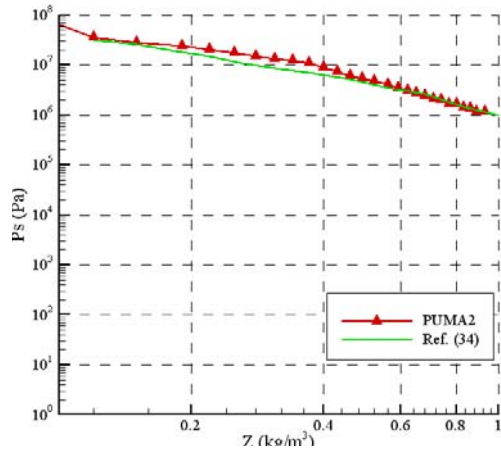


Figure 5. Variation of over-pressure with scaled distance. (Explosion of 75 lbs of TNT in free air).

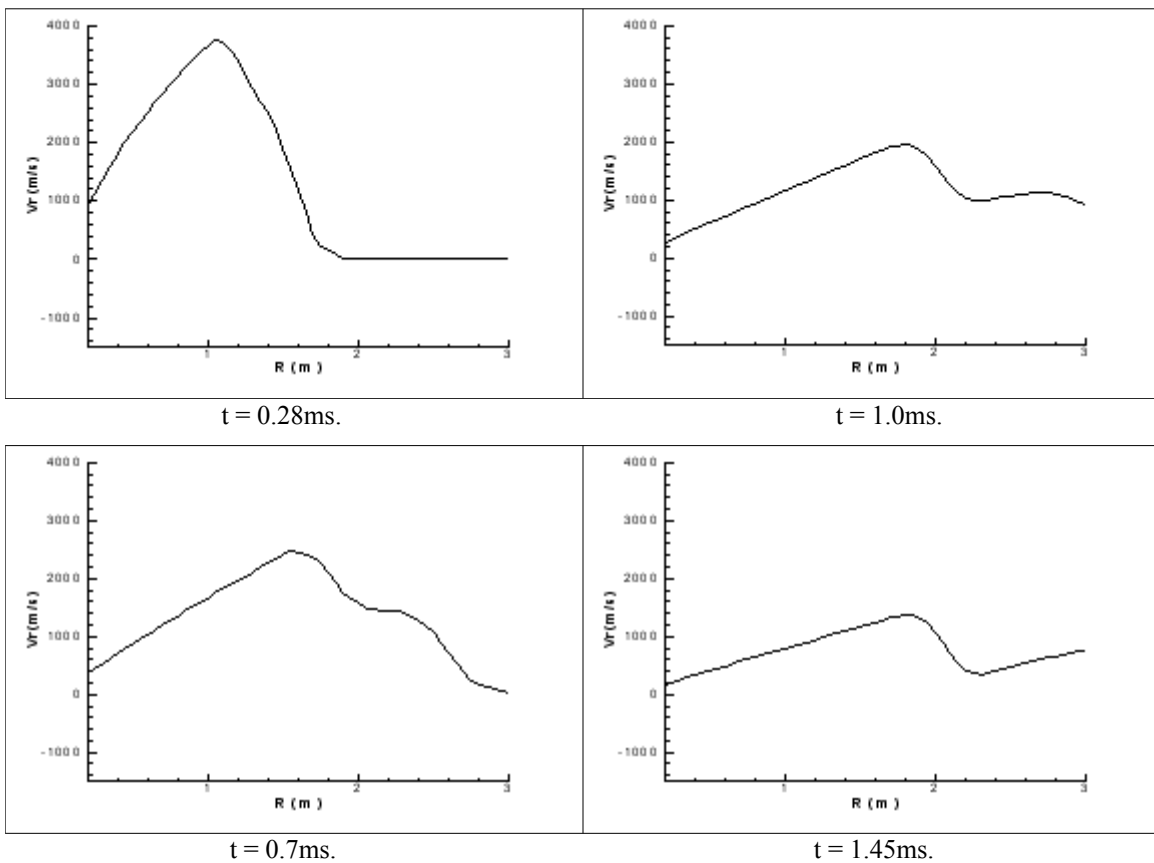


Figure 6. Variation of radial velocity with distance from the center of the explosive at different times

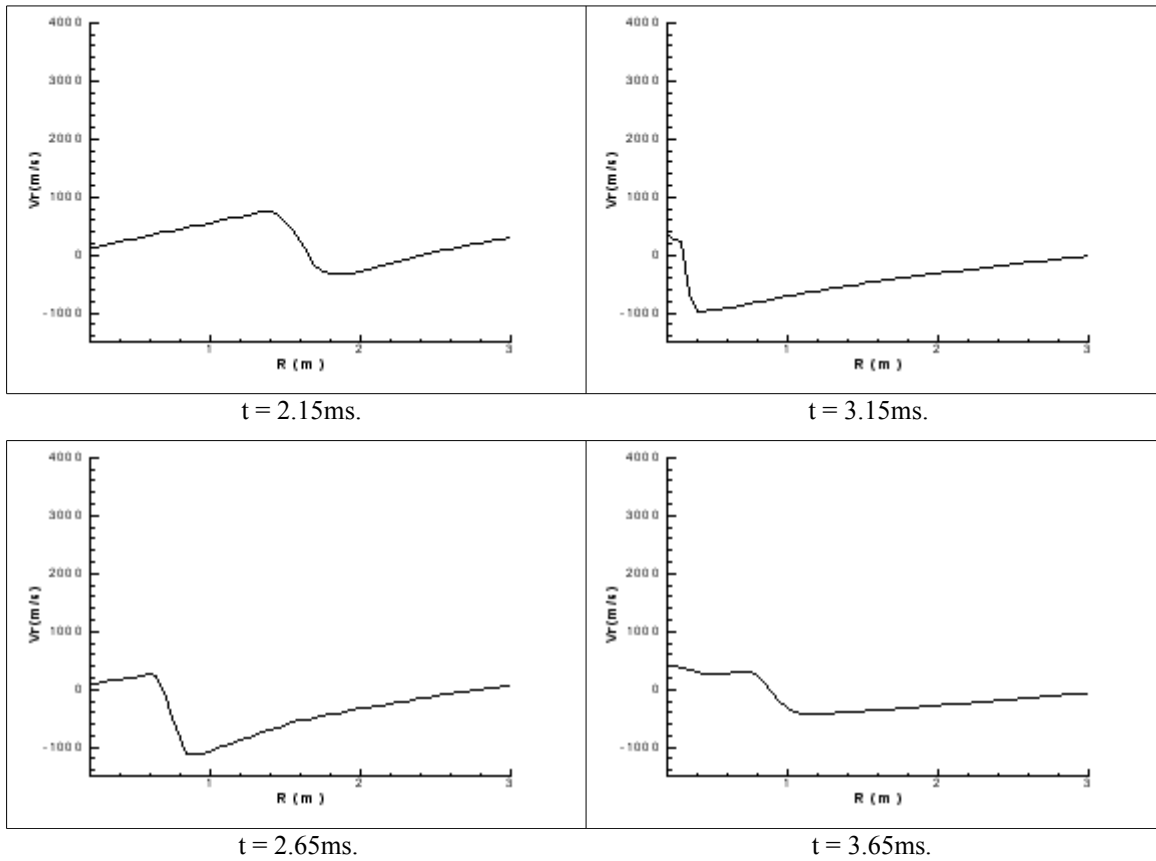


Figure 6. Variation of radial velocity with distance from the center of the explosive at different times. (continued)

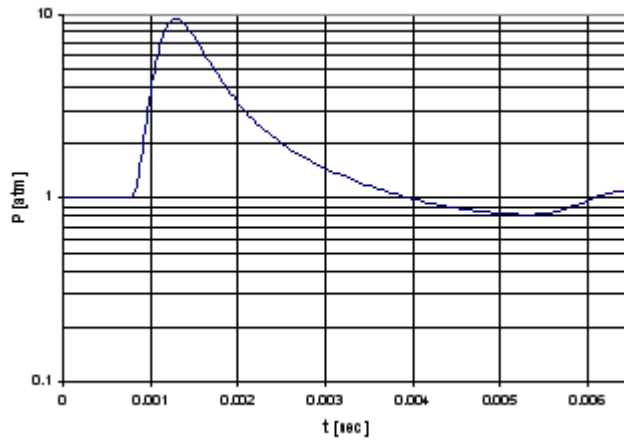


Figure 7. Pressure profile at $Z = 1$ (~3.24 m).

C. Blast Loading on a Square Plate

Finally the code was used to obtain blast loading on a square plate. Here, a 60 in. by 60 in. plate was placed 3.2 ft. away from 75 lbs. of TNT. Just like the previous case the explosive was assumed to be spherical in shape but this time the distance to the plate was measured from the surface of the explosive. Numerical solutions were performed for air with local equilibrium conditions to include high temperature effects. Figure 8 shows the side views of the pressure contours obtained at different times. The plate can be viewed as a black vertical line at the right side of the domain. This figure clearly shows the evolution of the spherical blast wave caused by the explosion, reflection of this shock from the plate, decrease in shock strength due to expansion, the negative phase, and the secondary shock occurred after the negative phase.

Pressure loading at the center of the plate is displayed in Figure 9. For comparison, results obtained using a calorically perfect gas assumption were also included in the graph. For this case the distance to the plate was measured from the center of the explosive rather than the surface. This difference between the solutions can be seen from the shock arrival times from Figure 9. The blue triangle shown in this figure corresponds to the peak pressure and shock arrival time obtained using A.T.-Blast software³⁶. Peak pressures obtained by equilibrium air and perfect gas solutions agree well with the A.T.-Blast predictions. There is a small discrepancy in the shock arrival time of the perfect gas solution but this is partly due to differences in distances from the explosives to the plate surface. It is clear from Figure 9 that high temperature effects had very little impact on the peak pressure. But the difference became obvious in the vicinity of the secondary shock where the equilibrium air solution predicted a sharper and stronger shock event. The after-shock behavior of this solution also yielded higher pressures.

Although pressure predictions obtained using equilibrium air and perfect gas solutions were not much different from each other, the temperature predictions differed considerably. Figure 10 shows the temperature history at the center of the plate obtained using these two solutions. As expected, the perfect gas solution yielded an unrealistically high peak temperature, which was more than twice the value predicted by the equilibrium air solution. This high temperature dropped very quickly to values lower than the predictions of the latter solution. The sharp secondary shock prediction of the equilibrium air solution is also visible in Figure 10. After this secondary shock both solutions gave similar temperature variations.

Pressure loading obtained using PUMA2 was used as input to the explicit finite element analysis code LS-DYNA to predict resultant stresses and displacements of an uncoated square, steel plate and a similar plate coated with polyurea. The plate is made of AISI 4340 steel with dimensions of 60" x 60" x 0.25". A coating thickness of 0.25 in. was used for the polyurea. The steel was modeled using a Johnson-Cook constitutive model;³⁷ a widely used model for metals at high-strain rate. The polyurea was modeled using a user-defined material model based on experimental data³⁸. The user-defined model provided a series of tables to represent constitutive relationships for various strain rates. Both the steel and polyurea incorporated failure criteria into the material models for fracturing predictions. For the failure criteria, strains at fracture observed from the experiment were used.

Figure 11 shows displacements at the center of the steel plate predicted by LS-DYNA. The steel plates without coating and with coating were both fully fractured at the edges at 1.05 ms and 1.21 ms into the blast event, respectively. The coated steel plate was able to sustain the applied pressure loads and avoided fragmentation; which did not occur for the uncoated plate. Despite its effectiveness against fragmentation, polyurea had little effect on the stiffness of the structure. The steel plates with and without coating both experienced a considerable amount of deformation during the blast event.

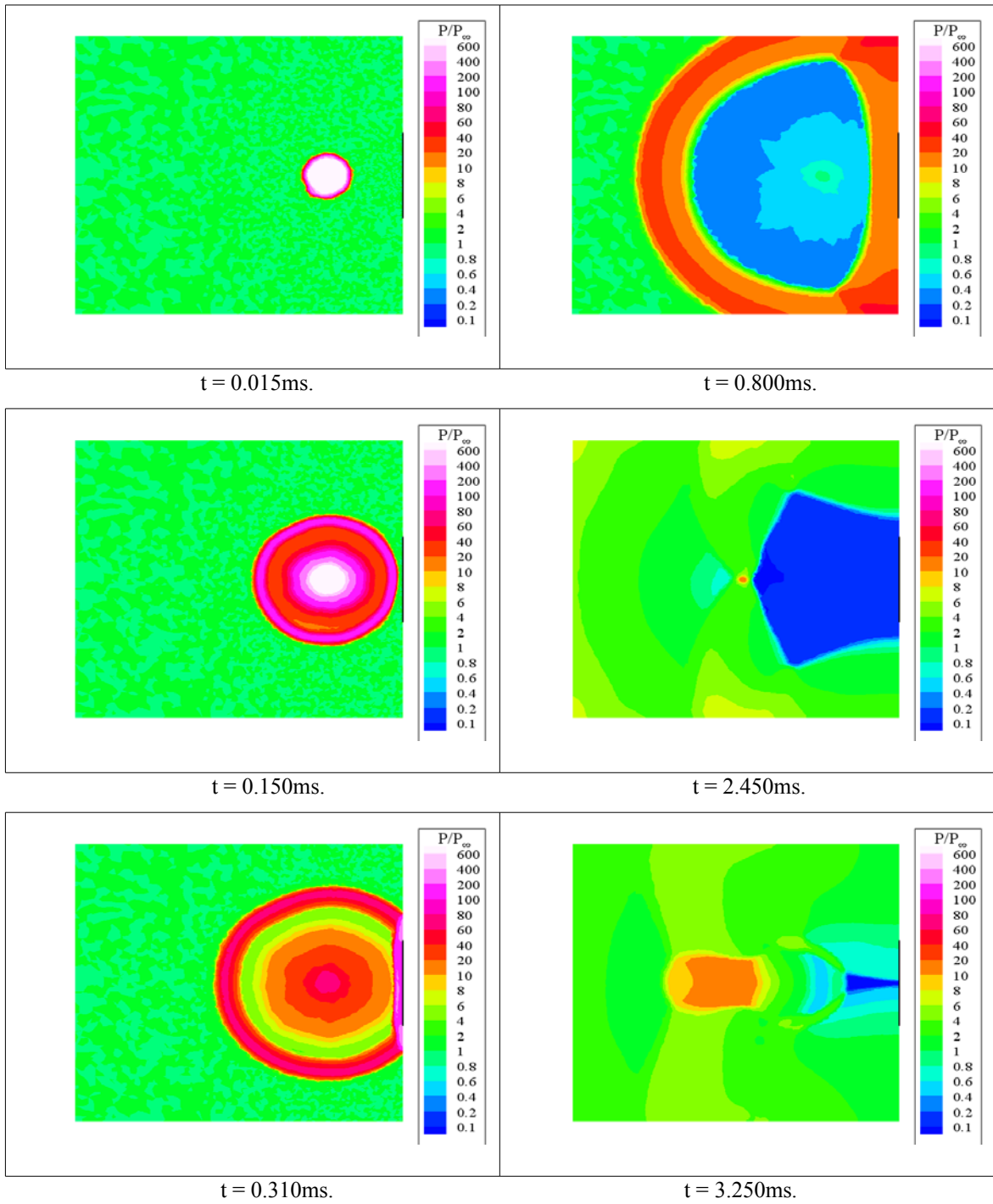


Figure 8. Pressure contours at different times. (side view)

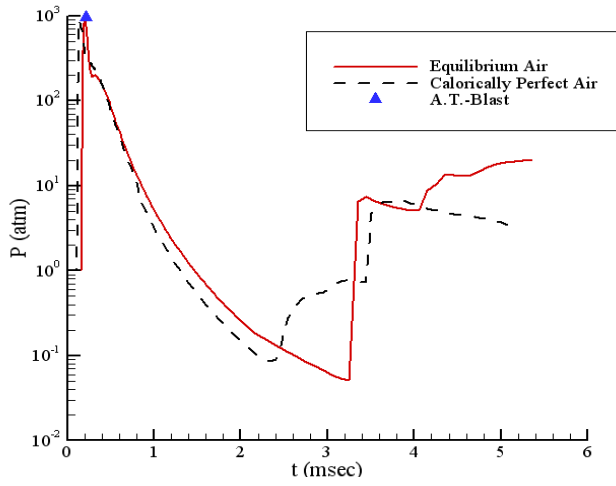


Figure 9. Pressure loading at the center of the plate.

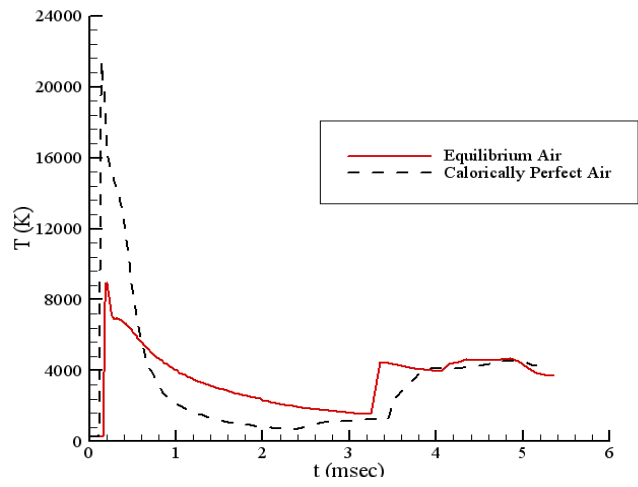


Figure 10. Temperature history at the center of the plate.

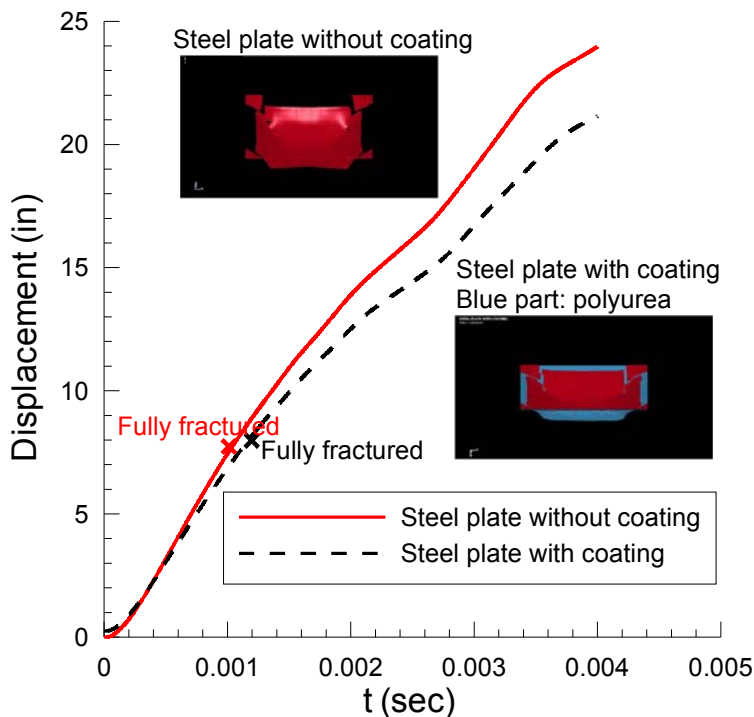


Figure 11. Vertical displacements at the center of the square plate.

V. Conclusions

The in-house Euler/Navier-Stokes solver PUMA2 was used to simulate blast waves caused by explosions and to predict blast loadings on a deformable square plate. Pressure loading obtained by PUMA2 was used as input for LS-DYNA to examine the effectiveness of polyurea for blast mitigation.

For accurate predictions PUMA2, which was originally designed to perform flow solutions for calorically perfect gases, was further modified to include high temperature effects. This was done by introducing new relations for γ , temperature and speed of sound for equilibrium air conditions²⁹. A new upwinding technique, AUSM⁺³¹, was also added to PUMA2 to perform solutions with high temperature effects.

For validation purposes PUMA2 was first tested for a planar shock wave - square cavity interaction problem. The density contours plotted at different times showed good agreement with the experimental results from Ref 32. After this, the code was used to simulate the evolution of a blast wave generated due to an explosion of 75 lbs of TNT in free air. In the solutions the explosive was assumed to be spherical in shape and the explosion was assumed to happen uniformly starting from the origin. Numerical simulations were started after the detonation wave reached the explosive surface and the effects are introduced to the flowfield as initial conditions according to Ref. 33. During the computations the air is assumed to be calorically perfect. The presence of the TNT products was also omitted for simplicity. Despite these assumptions PUMA2 was able to predict the peak over-pressure with good accuracy.

Finally the code was used to predict blast loading on a 60 in. by 60 in. steel plate placed 3.2 ft. away from 75 lbs of TNT. Simulations were performed for more than 5 ms and pressure loadings are used as input for LS-DYNA. Predictions were performed for air at local chemical equilibrium and air as a calorically perfect gas and were compared to peak pressure predictions from A.T.-Blast. PUMA2 predictions showed very good agreement with A.T.-Blast. Although pressure histories obtained by equilibrium air and perfect gas solutions were not much different, their temperature predictions differed considerably. The peak temperature of the calorically perfect gas solution was more than twice the value predicted by the solution with high temperature effects.

Results from the LS-DYNA simulations showed that the coating successfully prevented fragmentation. However, the coating was not very effective for increasing structural stiffness.

Acknowledgements

This research was funded by grant no. ONR N00014-05-1-0844.

References

1. Fickett W., "Introduction to Detonation Theory," University of California Press, 1985.
2. Dewey, J. M., "Expanding Spherical Shocks (Blast Waves)," *Handbook of Shock Waves*, Vol.2, 2001, pp. 441 – 481.
3. Sharma, A., Long, L. N., "Numerical Simulation of the Blast Impact Problem using the Direct Simulation Monte Carlo (DSMC) Method," *Journal of Computational Physics*, Vol. 200, 2004, pp. 211 – 237.
4. Long, L. N., Anderson, J. B., "The simulation of Detonations using a Monte Carlo Method," *Rarefied Gas Dynamics Conference*, Sydney, Australia, 200.
5. Anderson, J. B., Long, L. N., "Direct Simulation of Pathological Detonations," *18th International Symposium on Rarefied Gas Dynamics*, Vancouver, Canada, 2002.
6. Anderson, J. B., Long, L. N., "Direct Monte Carlo Simulation of Chemical Reaction Systems: Prediction of Ultrafast Detonations," *Journal of Chemical Physics*, Vol. 118, No. 7, 2003, pp. 3102 – 311.
7. O'Connor, P. D., Long, L. N., and Anderson J. B., "The Direct Simulation of Detonations," Invited Paper, AIAA 2006-4411, AIAA/ASME/SAE/ASEE Joint Propulsion Conference, Sacramento, CA, July, 2006
8. Sharma, A., Long L. N., Krauthammer, T., "Using the Direct Simulation Monte Carlo Approach for the Blast-Impact Problem," *The 17th International Symposium on Military Aspects of Blast Simulations*, Las Vegas, NV, 2002.
9. LS-DYNA Theory Manual, Livermore Software Technology Corporation.
10. Bruner, C. W. S., "Parallelization of Euler Equations on Unstructured Grids," Ph.D. Thesis, Virginia Polytechnic State and University, May 1996.
11. Hansen, R. P., Long, L. N., Large Eddy Simulation of a Circular Cylinder on Unstructured Grids," AIAA 2002-0982, Reno NV, January 2002.
12. Souliez, F. J., "Parallel Methods for Computing Unsteady Separated Flows Around Complex Geometries," Ph.D. Thesis, The Pennsylvania State University, Aerospace Engineering Department, August 2002.
13. Alpman, E., Long, L. N., Kothmann B. D., "Toward a Better Understanding of Ducted Rotor Antitorque and Directional Control in Forward Flight," *AHS 59th Annual Forum and Display*, Phoenix, AZ, May 2003.
14. Alpman, E., Long, L. N., "Unsteady RAH-66 Comanche Flowfield Simulations including Fan-in-Fin," AIAA Paper 2003-4231, *AIAA 16th CFD Conference*, Orlando, FL, June 2003.
15. Alpman, E., Long, L. N., Kothmann, B. D., "Understanding Ducted Rotor Antitorque and Directional Control Characteristics, Part I: Steady State Simulation," *Journal of Aircraft*, Vol.41, No 5, 2004, pp 1042 – 1053.
16. Alpman, E., Long, L. N., Kothmann, B. D., "Understanding Ducted Rotor Antitorque and Directional Control Characteristics, Part II: Unsteady Simulation," *Journal of Aircraft*, Vol.41, No 6, 2004, pp 1370 – 1378.
17. Modi, A., Long, L. N., Sezer-Uzol, N., Plassmann P., "Scalable Computational Steering System for Visualization of Large-Scale CFD Simulations," AIAA 2002-2750, *AIAA Fluids Conference*, St. Louis, June, 2002.
18. Souliez, F., Long, L., N., Morris, P. J., Sharma, A., "Landing Gear Aerodynamic Noise Prediction using Unstructured Grids," *International Journal of Aeroacoustics*, Vol. 1, (2), 2002.
19. Modi, A., "Unsteady Separated Flow Simulations Using a Cluster of Work Stations," M.S. Thesis, Penn State University, Aerospace Engineering Department, May 1999.
20. Modi, A., Long, L. N., "Unsteady Separated Flow Simulations using a Cluster of Workstations," AIAA 2000-0272, *38th AIAA Aerospace Sciences Meeting and Exhibit*, January, 2000.
21. Modi, A., Long, L. N., Plassmann, P. E. , "Real-Time Visualization of Wake-Vortex Simulations using Computational Steering and Beowulf Clusters," *VECPAR*, Portugal, June 2002.
22. Long, L. N., Modi, A., "Turbulent Flow and Aeroacoustics Simulations using a Clusters of Workstations," *NCSA Linux Revolution Conference*, Illinois, June, 2001.
23. Sharma, A., Long, L. N., "Airwake Simulations on an LPD 17 Ship," AIAA 2001-2589, *AIAA 15th CFD Conference*, Anaheim, CA, June, 2001.
24. Long, L. N. Souliez F., Sharma, A., "Aerodynamic Noise Prediction using Parallel Methods on Unstructured Grids," AIAA 2001-2196, *7th AIAA/CEAS Aeroacoustics Conference*, Maastricht, Netherlands, May 2001.
25. Schweitzer, F., "Computational Simulation of Flow around Helicopter," M.S. Thesis, Penn State University, Aerospace Engineering Department, May 1999.
26. Hansen R., "Separated Turbulent Flow," Ph.D. Thesis, Penn State University, Mechanical Engineering Department, August 2001.
27. Anderson, J. D., "Hypersonic and High Temperature Gas Dynamics," McGraw-Hill, Inc., 1989.
28. Hoffman, K. A., Chiang, S. T., "Computational Fluid Dynamics, Volume II," Engineering Education System, 2000.
29. Tannehill, J. C., and Mugege P. H., "Improved Curve Fits for the Thermodynamic Properties Equilibrium Air Suitable for Numerical Computation using Time Dependent and Shock-Capturing Methods," NASA CR-2470, 1974.
30. Roe, P. L., "Approximate Riemann Solvers, Parameter Vectors and Difference Schemes," *Journal of Computational Physics*, Vol. 43, 1981, pp. 357 – 372.

31. Liou, M. -S., "A sequel to AUSM: AUSM+," *Journal of computational Physics*, Vol. 129, 1996, pp. 364 – 382.
32. Igra, O., Falcovitz, J., Reichenbach, H., Heilig, W., "Experimental and Numerical Study of Interaction between a Planar Shock Wave and a Square Cavity," *Journal of Fluid Mechanics*, vol. 313, 1996, pp. 105 – 130.
33. Taylor, G., "The dynamics of the Combustion Products behind Plane and Spherical Detonation Fronts in Explosives," *Proceedings of the Royal Society of London. Series A, Mathematical and Physical Sciences*, Vol. 200, No. 1061, 1950, pp. 235 – 247.
34. Smith, P. D., Hetherington J. D., "*Blast and Ballistic Loading of Structures*," Butterworth-Heinemann, 1994, pp. 36.
35. Brode, H. L., "Blast Wave from a Spherical Charge," *The Physics of Fluids*, Vol. 2 (2), 1959, pp. 217 – 229.
36. AT-Blast 2.2, Applied Research Associates, Inc.
37. Kurtaran, H., Eskandarian A., "Design Automation of a Laminated Armor for Best Impact Performance using Approximate Optimization Method," *The International Journal of Impact Engineering*, Vol. 29, pp. 397 – 406.
38. Roland, C.M., Twigg, J.N., Vu Y., Mott P.H., "High Strain Rate Mechanical Behavior of Polyurea," *Polymer*, Vol. 48, pp. 574 - 578.